

Coordination defects in bismuth-modified arsenic selenide glasses: High-resolution x-ray photoelectron spectroscopy measurements

Roman Golovchak,^{1,2} Oleh Shpotyuk,^{2,3} Andriy Kovalskiy,¹ Alfred C. Miller,¹ Jiří Čech,¹ and Himanshu Jain^{1,*}

¹*Department of Materials Science and Engineering, Lehigh University, 5 E. Packer Avenue, Bethlehem, Pennsylvania 18015-3195, USA*

²*Lviv Scientific Research Institute of Materials of SRC “Carat,” 202 Stryjska Street, Lviv UA-79031, Ukraine*

³*Institute of Physics of Jan Dlugosz University, 13/15, al. Armii Krajowej, Czestochowa, 42201, Poland*

(Received 7 April 2008; published 14 May 2008)

The possibility of coordination defects formation in Bi-modified chalcogenide glasses is examined by high-resolution x-ray photoelectron spectroscopy. The results provide evidence for the formation of positively charged fourfold coordinated defects on As and Bi sites in glasses with low Bi concentration. At high Bi concentration, mixed $\text{As}_2\text{Se}_3\text{-Bi}_2\text{Se}_3$ nanocrystallites are formed in the investigated Se-rich As-Se glasses.

DOI: [10.1103/PhysRevB.77.172201](https://doi.org/10.1103/PhysRevB.77.172201)

PACS number(s): 61.43.Fs, 82.80.Pv, 71.23.Cq, 79.60.-i

The existence of coordination defects (CDs) such as the pairs of positively charged overcoordinated and negatively charged undercoordinated atoms in covalently bonded chalcogenide glasses (ChGs) is one of the most controversial points in glass science.^{1–11} To explain the unique features of these semiconducting materials, the earliest electronic band-gap models^{4–9} assumed a high density ($\sim 10^{17} - 10^{20} \text{ cm}^{-3}$) of defect energetic states, which pin the Fermi level near the middle of the gap. Consequently, it is difficult to change the type of conductivity such as from *p* type to *n* type by conventional doping with aliovalent impurities. Since 1975, various authors have proposed with variable success these defect states as due to dangling bonds,^{5–7} CDs,^{8,9} or “wrong” homopolar bonds (chemical disorder).¹⁰ Among them, the CDs provide the most attractive explanation for the unique photoinduced phenomena exhibited by ChG. However, convincing experimental evidence for the existence CD in virgin ChG structure has not been obtained thus far. Reasons for the lack of their observation include diamagnetic nature of CDs, or perhaps their low intrinsic concentration at the level of $\sim 10^{17} \text{ cm}^{-3}$.^{1,11} Therefore, traditional experimental techniques used for defect detection in solids, viz., electron spin resonance, nuclear magnetic resonance, and Raman and infrared (IR) vibrational spectroscopies are not useful for detecting intrinsic or *native* CDs in ChG.^{1,7} Only indirect evidence for *transient* CDs induced by *in situ* photoexposure at low temperatures has been obtained with extended x-ray absorption fine structure spectroscopy for some Se-based ChG.¹² Additionally, the formation of *metastable* CDs caused by high-energy irradiation^{13,14} or photoexposure¹⁵ has been inferred from the analysis of IR vibrational spectra that show switching of covalent bonds.

Recently, it was proposed that the addition of Bi introduces high concentration of native CDs into the network of Se-based ChG and changes their electrical conductivity from *p* to *n* type.^{16,17} This experimental observation has opened broad opportunities for the application of ChG, since in the past they were found to possess only *p*-type electrical conductivity that was insensitive to doping.^{1,7} However, the role of Bi in transforming electrical conduction from *p* type to *n* type remains ambiguous. According to one model, Bi atoms are incorporated into chalcogen-based network as positively charged centers (both Bi_3^+ or Bi_4^+ CD, where superscript means charge state and subscript means coordination),^{18,19}

while others have suggested negatively charged defect centers (Bi_2^- or Bi_6^- CD).^{17,20} Yet other authors consider Bi as electronic analog of As and Sb atoms to form pyramidal structural units $\text{BiSe}_{3/2}$ of normal coordination, such as $\text{As/SbSe(S)}_{3/2}$ pyramids predicted by “8-N” rule.^{1,21,22} Each of these approaches provides its own explanation of changes in electrical conductivity from *p* to *n* type, which is applicable only for some specific ChG compositions (close to stoichiometry²²) or systems [such as Ge-Bi-Se/S (Refs. 16 and 18)].

In this work, we have exploited high-resolution x-ray photoelectron spectroscopy (XPS) to establish the role of Bi in the structure of typical Se-rich glasses, such as As-Se. Specifically, we have investigated changes introduced by a small addition (up to 4 at. %) of Bi in the electronic subsystem of $\text{As}_{20}\text{Se}_{80}$ ChG of eutectic composition.²³ We have chosen the compositions with due consideration to the glass forming region of As-Se-Bi system,^{1,23} the sensitivity of XPS technique and to the predicted concentration of CD (couple of percents¹⁶).

The bulk ChG samples were prepared by conventional melting of appropriate mixture of high purity (99.999%) precursors in evacuated quartz ampoules, followed by air quenching to room temperature.

The XPS spectra were recorded with a Scienta ESCA-300 spectrometer using monochromatic $\text{Al K}\alpha$ X-ray (1486.6 eV). The instrument was operated in a mode that yielded a Fermi-level width of 0.4 eV for Ag metal and at a full width at half maximum (FWHM) of 0.54 eV for Ag $3p_{5/2}$ core-level peak. Energy scale was calibrated using the Fermi level of clean Ag. To eliminate ambiguities that might be introduced into the XPS spectra as a result of surface reactions with oxygen or other surface contamination, the glass specimens were fractured inside the analysis chamber at pressures typically 2×10^{-8} mbar or less. The surface charging from photoelectron emission was controlled by flooding the surface with low-energy (< 10 eV) electrons. The raw data were calibrated according to the gold $4f_{7/2}$ (84 eV) line position, as described elsewhere.²⁴

Data analysis was conducted with standard CASA-XPS software package. For analyzing the core-level spectra, Shirley background was subtracted and a Voigt line shape was assumed for the peaks.²⁵ Each *d* core-level spectrum for As, Bi, and Se in our samples consisted of one or more spin orbit

doublets splitting into $d_{5/2}$ and $d_{3/2}$ components. The number of doublets within a given peak was determined by an iterative curve fitting process in which a doublet was added only if it significantly improved the goodness of fit of the experimental data to the envelope of the fitted curve. The uncertainties in the peak position and area of each component were ± 0.05 eV and $\pm 2\%$, respectively.

Recently, we have demonstrated the usefulness of XPS technique to identify gamma-induced metastable CDs in radiation-modified S-based ChG.²⁶ In general, the identification procedure is based on the main principle of XPS data analysis²⁷ that the position (or binding energy) of a core-level XPS peak of a given atom would shift with respect to normal position as a result of the following:

(I) changes in its coordination (higher/lower number of nearest neighbors),

(II) changes in the ionic state (changes in bond type, excess of positive/negative charge, etc.), and

(III) substitution of one or more of its neighbors by a chemical element with different electronegativities or charge states (charged defects, etc.).

So, if over- or undercoordinated charged defects form in the covalent network, we should observe (according to I and II) additional doublets in the XPS core-level spectrum of a given element related to its specific defects (i.e. As_4^+ , Bi_4^+ , Se_3^- , or Se_3^+) and additional doublets associated with the influence of these defects on the neighbored atoms (according to III). It should be noted here that the formation of nanocrystallites can also shift the position of core-level peak compared to its position in glass, as reported by Takahashi *et al.*²⁸ For this reason, we have included a partially crystallized sample of $\text{As}_{20}\text{Se}_{76}\text{Bi}_4$ composition in our study.

Differential scanning calorimetry data of all investigated ChG showed the presence of glassy phase in all samples including the partially crystallized composition. No large-scale phase separations or cluster formation could be inferred from these data. X-ray diffraction (XRD) spectra showed the presence of crystallites only in the sample of $\text{As}_{20}\text{Se}_{76}\text{Bi}_4$ composition. The peaks in the XRD pattern of this specimen correspond to the reflections of hexagonal phase similar to the one observed for Bi_2Se_3 nanocrystals.²⁹ All the remaining samples did not show any significant crystalline reflections in their XRD patterns. Scanning electron micrographs (SEMs) of the present samples confirm this observation. For example, freshly fractured surfaces of $\text{As}_{19}\text{Se}_{80}\text{Bi}_1$ and $\text{As}_{20}\text{Se}_{76}\text{Bi}_4$ samples are compared in Fig. 1. The vortexlike structures, which were uniformly distributed throughout the whole bulk of the $\text{As}_{20}\text{Se}_{76}\text{Bi}_4$ sample [Fig. 1(b)], were not observed in any other investigated composition. No elements other than the glass components were observed in the survey XPS spectra, which showed only peaks associated with the As, Bi, and Se core levels and related Auger lines. In particular, there was no evidence for oxygen or sulfur contaminations on any of the surfaces.

The XPS 3d core-level spectra of As and Se in Bi-free samples can be fitted by the number of doublets predicted by the “chains crossing model,” which was recently validated for As-Se ChG.²⁴ According to this model, the $\text{As}_{20}\text{Se}_{80}$ ChG contains only Se-Se-Se (25%), As-Se-Se (75%), and Se-As < (Se)₂ (100%) structural units.²⁴ Experimentally obtained

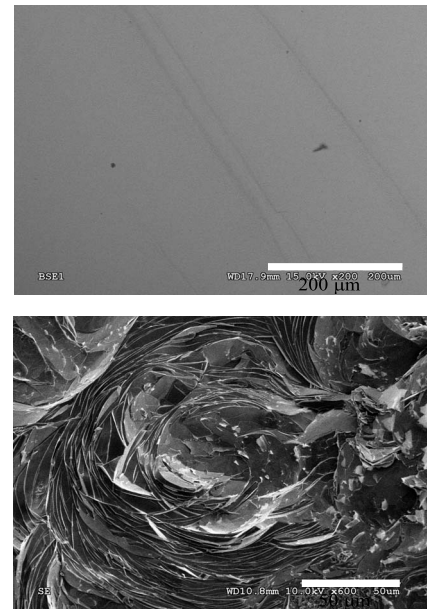


FIG. 1. SEM images of freshly generated cracks in (a) $\text{As}_{19}\text{Se}_{80}\text{Bi}_1$ (backscattered electron image) and (b) $\text{As}_{20}\text{Se}_{76}\text{Bi}_4$ (secondary electron image) ChGs.

As and Se 3d core-level spectra for $\text{As}_{20}\text{Se}_{80}$ ChG and their best fits are presented in Fig. 2(a). Fitting parameters, such as peak position or binding energy, partial area (A), and FWHM are given in the insets of Fig. 2. On the basis of electronegativity data and compositional dependence of XPS spectra in this ChG system,²⁴ the Se 3d doublets with the intensity of primary components at ~ 54.8 eV were attributed to Se-Se-Se, at ~ 54.4 eV to As-Se-Se and at ~ 54.0 eV to As-Se-As structural fragments (Fig. 2). The As 3d doublet with the intensity of main component at ~ 42.1 eV was assigned to Se-As < (Se)₂ regular environment (Fig. 2). There is no evidence for the existence of charged over- and/or undercoordinated atoms in observable concentrations (more than the detection limit of the technique, i.e., a couple of percent) according to the present analysis of XPS core-level spectra of Bi-free bulk ChG.

This situation changes with Bi addition [Figs. 2(b) and 2(c)]. Besides the doublet at ~ 42.1 eV of Se-As < (Se)₂ regular environment, additional doublets appear on the high-energy side of the As core level for $\text{As}_{19}\text{Se}_{80}\text{Bi}_1$. The doublet at ~ 43.0 eV, a characteristic ChG with low Bi concentration (less than 1 at. %), becomes insignificant (less than $\sim 2\%$ of the whole area under XPS As core-level spectra) with increasing Bi concentration, while the one at ~ 42.4 eV becomes dominant ($\sim 97\%$ of all As atoms) in $\text{As}_{20}\text{Se}_{76}\text{Bi}_4$ composition. Additionally, for the latter ChG, the chemical shift between Se and As core-level XPS spectra decreases on ~ 0.2 eV in comparison to the Bi-free samples for which XPS core-level spectra exhibit almost constant shift of ~ 12.2 eV independent of composition.²⁴ A similar behavior was observed earlier for As_2Se_3 glasses doped with > 4 at. % Bi,³⁰ which could not be explained.

The doublet in As core level with primary component at ~ 43.0 eV [Fig. 2(b)] is assigned to the formation of As_4^+ coordination defects according to the above principle of CD

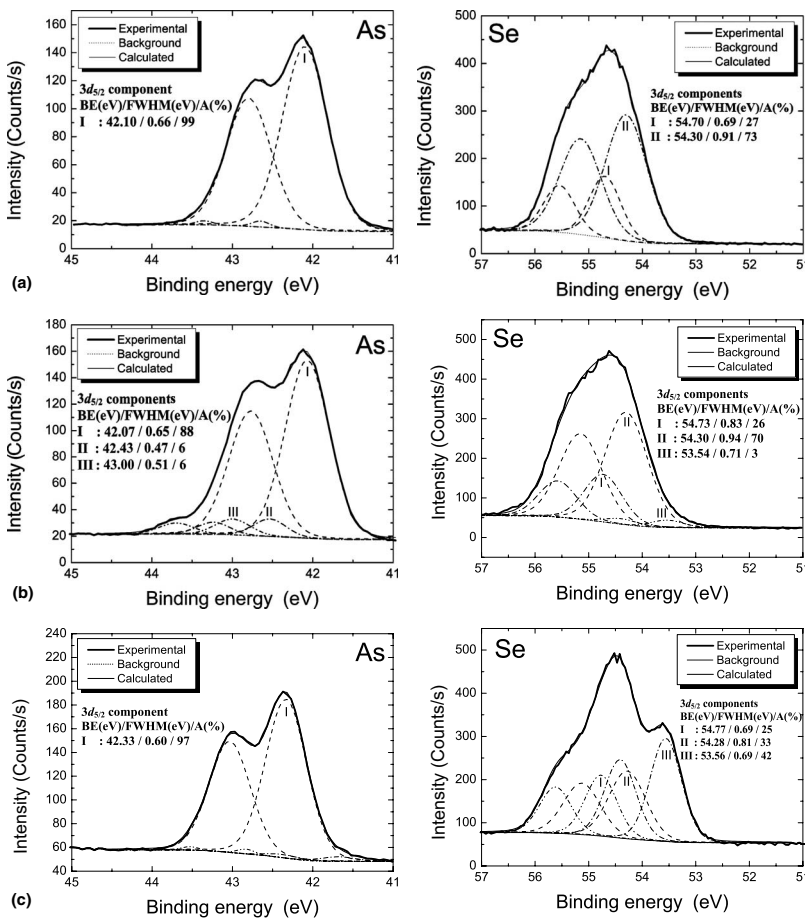


FIG. 2. Fitting of As and Se 3d core-level spectra for $\text{As}_{20}\text{Se}_{80}$ (a), $\text{As}_{19}\text{Se}_{80}\text{Bi}_1$ (b), and $\text{As}_{20}\text{Se}_{76}\text{Bi}_4$ (c) samples. A, the ratio, experimentally obtained by XPS as partial area under corresponded fitted peaks.

identification, while the component at ~ 42.4 eV is suggested as due to the As atoms that take part in the formation of mixed Bi_2Se_3 - As_2Se_3 nanocrystallites of hexagonal structure. It was shown on the basis of XRD and optical investigations that the incorporation of As into Bi_2Se_3 crystalline structure does not significantly change the lattice parameters of the latter.³¹ The increase in the binding energy of As 3d core-level of nanocrystalline phase (42.4 eV) in comparison to the one of glass (42.1 eV for $\text{As}_{20}\text{Se}_{80}$ ChG) can be explained by the increase in the ionicity of As-Se bond during nanocrystallite formation. This leads to a high-energy shift of As 3d and low-energy shift of Se 3d core level for the $\text{As}_{20}\text{Se}_{76}\text{Bi}_4$ ChG because of a charge transfer from As atoms toward Se atoms [note the respective electronegativities are $\chi_{\text{Se}}=2.55$, $\chi_{\text{As}}=2.18$, $\chi_{\text{Bi}}=2.02$ (Ref. 32)]. This explanation is similar to that offered by Takahashi *et al.*²⁸ to explain the ~ 0.4 eV decrease in the BE of Se 3d peaks in Bi_2Se_3 crystal compared to the glass of the same composition.

The 4f and 5d doublets in the core-level spectra of Bi are very well resolved (5.3 eV and 3.0 eV, respectively³³) that allows us to clearly distinguish two different sites of Bi in the samples with low concentration (e.g., $\text{As}_{19}\text{Se}_{80}\text{Bi}_1$ ChG), while only one site is resolved in ChG samples with Bi concentration greater than 2 at. % ($\text{As}_{20}\text{Se}_{76}\text{Bi}_4$ ChG, for example). Because the broad peaks of Se 3p electrons (doublet with primary component at ~ 161 eV) hinder the analysis of Bi 4f XPS core-level spectra, we use Bi 5d XPS spectra for further quantitative characterization (insets of Fig. 3).³³ From the position of primary component in the 5d XPS core-level

spectrum for glassy (~ 25.1 eV) and crystalline (~ 25.0 eV) Bi_2Se_3 ,²⁸ the observed doublet with primary component at the low-energy side (~ 24.9 eV) is attributed to threefold coordinated Bi atoms. The other doublet with primary component at ~ 25.7 eV (Fig. 3) should correspond to Bi atoms with higher coordination or positively charged centers. So on the basis of this simple result, we can conclude that at low concentrations Bi enters the glass network in the form of positively charged defect centers and provides experimental evidence for the models proposed in Refs. 16, 18, and 19. Increase in Bi concentration initiates the devitrification of initial glass matrix and, finally, to the formation of nanocrystallites.

The present analysis favors the formation of Bi_4^+ CDs rather than $\text{Bi}_3^{\delta+}$ centers (δ represents the degree of ionicity of the covalent bond) considered in $\text{Bi}_x\text{Ge}_{20}\text{S}_{80-x}$ ChG with $3 < x < 10$.¹⁸ According to Ref. 28, an increase in the ionicity of Bi-Se bond causes an increase in the Bi 5d XPS core-level energy by ~ 0.1 eV. The observed difference between the two doublets of Bi 5d core level for $\text{As}_{19}\text{Se}_{80}\text{Bi}_1$ ChG is ~ 0.8 eV, which suggests changes in both the coordination and the charge states of Bi atoms.

The addition of Bi affects the Se 3d XPS core-level spectra too [Figs. 2(b) and 2(c)]. Besides the doublets of regular structural units expected from the chains crossing model,²⁴ curve fitting indicates the presence of additional doublet on the low-energy side of the primary component at ~ 53.5 eV [Figs. 2(b) and 2(c)]. This component becomes more significant with increasing Bi concentration in the samples. The

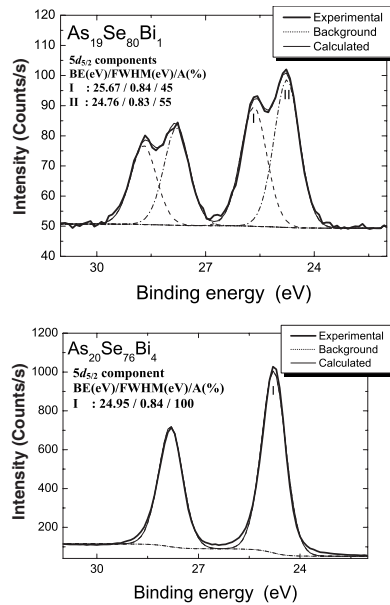


FIG. 3. Fitting of Bi 5d core-level spectra for selected Bi-modified glasses.

additional doublet in Se 3d XPS core-level spectrum speaks in favor of an increase in the ionicity of Se-As bonds, similar to that mentioned above with the formation of nanocrystallites (Bi/As-Se-As/Bi complexes). However, the existence of As_4^+ and Bi_4^+ coordination defects [as found from As and Bi core-level spectra, Figs. 2(b) and Fig. 3] should lead to

the existence of negatively charged Se_1^- defect centers to maintain electroneutrality of the samples. So, the observed component on the low-energy side of Se 3d core-level spectra of ChG with low Bi concentration could be also attributed to the existence of these defects. Unfortunately, it is difficult to resolve signals corresponding to Se in these two configurations due to the low concentration of Se_1^- defects (relative to the total concentration of Se atoms). Conversion of certain amount of Se-Se-As units into Se-Se-Se and As-Se-As units can be also inferred from the analysis of data for $As_{19}Se_{80}Bi_1$ and, especially, for the $As_{20}Se_{76}Bi_4$ composition [Figs. 2(b) and 2(c)]. The latter is equivalent to $As_{24}Se_{76}$ composition (with regard to Se content) and therefore should mostly consist of pyramids corner shared via the Se-Se bond.²⁴ The presence of As_4^+ or Bi_4^+ defects in the structure of $As_{19}Se_{80}Bi_1$ ChG should increase the FWHM of the Se 3d core-level peaks, as observed experimentally (insets of Fig. 2).

In conclusion, the analysis of core-level XPS spectra supports previously proposed models that the addition of Bi into Se-rich network of As-Se ChG in low concentration (approximately up to 1 at. %) stimulates the formation of coordination defect pairs $Bi_4^+Se_1^-$ and $As_4^+Se_1^-$ in concentration $10^{19}-10^{20} \text{ cm}^{-3}$. Increase in Bi concentration leads to the formation of mixed As_2Se_3 - Bi_2Se_3 nanocrystallites.

The authors thank the U.S. National Science Foundation, through the International Materials Institute for New Functionality in Glass (IMI-NFG), for providing partial financial support for this work (NSF Grant No. DMR-0409588). The authors are grateful to Bill Heffner for useful discussions.

*h.jain@lehigh.edu

- ¹A. Feltz, *Amorphous Inorganic Materials* (VCH, Weinheim, 1993), p. 446.
- ²Yu. M. Galperin, V. G. Karpov, and V. I. Kozub, *Adv. Phys.* **38**, 669 (1989).
- ³S. I. Simdyankin *et al.*, *Phys. Rev. Lett.* **94**, 086401 (2005).
- ⁴M. Cohen, H. Fritzsche, and S. Ovshinsky, *Phys. Rev. Lett.* **22**, 1065 (1969).
- ⁵R. A. Street and N. F. Mott, *Phys. Rev. Lett.* **35**, 1293 (1975).
- ⁶N. F. Mott, E. A. Davis, and R. A. Street, *Philos. Mag.* **32**, 961 (1975).
- ⁷N. F. Mott and E. A. Davis, *Electron Processes in Non-Crystalline Materials* (Clarendon, Oxford, 1979), p. 368.
- ⁸M. Kastner, D. Adler, and H. Fritzsche, *Phys. Rev. Lett.* **37**, 1504 (1976).
- ⁹M. Kastner, *J. Non-Cryst. Solids* **31**, 223 (1978).
- ¹⁰Ke. Tanaka, *J. Optoelectron. Adv. Mater.* **3**, 189 (2001).
- ¹¹G. J. Adriaenssens and N. Qamhieh, *J. Mater. Sci.: Mater. Electron.* **14**, 605 (2003).
- ¹²A. V. Kolobov, H. Oyanagi, K. Tanaka, and Ke. Tanaka, *Phys. Rev. B* **55**, 726 (1997).
- ¹³R. Golovchak and O. Shpotyuk, *Philos. Mag.* **85**, 2847 (2005).
- ¹⁴O. I. Shpotyuk, *Phys. Status Solidi B* **183**, 365 (1994).
- ¹⁵L. Tichy *et al.*, *Opt. Mater. (Amsterdam, Neth.)* **10**, 117 (1998).
- ¹⁶C. Vautier, *Solid State Phenom.* **71**, 249 (2000).
- ¹⁷N. Tohge, T. Minami, Y. Yamamoto, and M. Tanaka, *J. Appl. Phys.* **51**, 1048 (1980).

- ¹⁸S. R. Elliott and A. T. Steel, *Phys. Rev. Lett.* **57**, 1316 (1986).
- ¹⁹J. M. Saiter, T. Derrey, and C. Vautier, *J. Non-Cryst. Solids* **77-78**, 1169 (1985).
- ²⁰K. I. Bhatia, *J. Non-Cryst. Solids* **54**, 173 (1983).
- ²¹L. Tichy, H. Ticha, A. Triska, and P. Nagels, *Solid State Commun.* **53**, 399 (1985).
- ²²J. C. Phillips, *Phys. Rev. B* **36**, 4265 (1987).
- ²³Z. U. Borisova, *Glassy Semiconductors* (Plenum, New York, 1981), p. 505.
- ²⁴R. Golovchak *et al.*, *Phys. Rev. B* **76**, 125208 (2007).
- ²⁵J. M. Conny and C. J. Powell, *Surf. Interface Anal.* **29**, 856 (2000).
- ²⁶A. Kovalskiy *et al.*, *J. Phys. Chem. B* **110**, 22930 (2006).
- ²⁷*Practical Surface Analysis*, edited by D. Briggs and M. P. Seah, 2nd ed. (Wiley, New York, 1990), Vol. 1, p. 483.
- ²⁸T. Takahashi, T. Sagawa, and H. Hamanaka, *J. Non-Cryst. Solids* **65**, 261 (1984).
- ²⁹S. Xu *et al.*, *Mater. Lett.* **59**, 319 (2005).
- ³⁰S. Kumar, S. Kashyap, and K. Chopra, *J. Appl. Phys.* **72**, 2066 (1992).
- ³¹A. Sklenar, C. Drasar, A. Krejcova, and P. Lostak, *Cryst. Res. Technol.* **35**, 1069 (2000).
- ³²L. Pauling, *The Nature of the Chemical Bond* (Cornell University Press, Ithaca, 1960) 664 p.
- ³³J. F. Moulder, W. F. Stickle, P. E. Sobol, and K. D. Bomben, *Handbook of X-ray Photoelectron Spectroscopy*, edited by J. Chastein (Perkin-Elmer Corp., Eden Prairie, MN, 1992).